

Self-Interacting Dark Matter Subhalos in the Milky Way's Tides

Omid Sameie,^{1,*} Hai-Bo Yu,¹ Laura V. Sales,¹ Mark Vogelsberger,² and Jesús Zavala³

¹*Department of Physics and Astronomy, University of California, Riverside, CA 92521 USA*

²*Department of Physics, Kavli Institute for Astrophysics and Space Research,
Massachusetts Institute of Technology, Cambridge, MA 02139, USA*

³*Center for Astrophysics and Cosmology, Science Institute,
University of Iceland, Dunhagi 5, 107 Reykjavik, Iceland*

We study evolution of self-interacting dark matter (SIDM) subhalos in the Milky Way (MW) tidal field. The interaction between the subhalos and the MW's tides lead to more diverse dark matter distributions in the inner region, compared to their cold dark matter counterparts. We test this scenario with two MW satellite galaxies, Draco and Fornax, opposite extremes in the inner dark matter content, and find they can be accommodated within the SIDM model proposed to explain the diverse rotation curves of spiral galaxies in the field.

Introduction. Dark matter makes up 85% of the mass in the universe, but its nature remains largely unknown. Over the past decades, most studies have focused on the cold dark matter (CDM) model, where the dark matter is composed of collisionless massive particles. CDM has a tremendous success in explaining the large-scale structure of the universe [1] and overall features of galaxy formation and evolution [2–4]. However, it has also long-standing issues in accommodating observations on galactic scales [5, 6]. For example, rotation curves of field spiral galaxies exhibit a great diversity, i.e., there is a large spread in the inner circular velocity for these systems at a fixed mass [7]. On the other hand, they also show a uniform feature: the total radial acceleration is correlated with the baryonic contribution [8]. Recently, it has been shown that both the diversity and uniformity can be reconciled in the self-interacting dark matter (SIDM) model with a fixed cross section [9]. In SIDM, dark matter collisions thermalize the inner halo over the cosmological timescale [10–15], together with the baryonic matter and correlate their distributions in a coherent way [16–22], in accord with observations of spiral galaxies in the field [23–25].

SIDM may also provide a solution to puzzles associated with dwarf spheroidal galaxies (dSphs) in the Milky Way (MW), e.g., the most massive subhalos predicted in CDM are too massive to host the bright MW dSphs [26, 27]. SIDM simulations show that dark matter self-interactions can lower the central density of the subhalos and alleviate the tension [14, 28]. Despite this success, a detailed analysis of stellar kinematics of the bright MW dSphs shows the preferred dark matter self-scattering cross section per mass, σ/m , varies within a wide range [29]. The spread in the cross section reflects diverse dark matter contents of MW dSphs' halos, beyond the scatter predicted in CDM-only simulations as in [30]. For example, Draco and Ursa Minor are much denser than Fornax and Sextans [29, 31–33]. Unlike spiral galaxies in the field, we expect environmental effects to play a relevant role in shaping MW subhalos. Indeed, in the case of CDM, the tidal effects can lower central

densities for massive subhalos [34–38] and reduce the number of small ones [39–42].

Cosmological simulations have shown that SIDM subhalos have a larger spread in the inner dark matter content for $\sigma/m = 10 \text{ cm}^2/\text{g}$ [14], compared to the CDM case. In particular, with such a large cross section, subhalos could experience SIDM core collapse, resulting in high central densities. More recently, it has been suggested that Draco's host could be in the core-collapse phase for $\sigma/m \gtrsim 5 \text{ cm}^2/\text{g}$ [43], as it has a small pericenter distance to the MW estimated from Gaia data [44] and the tidal effect could trigger the core collapse. Intriguingly, for the bright MW dSphs, there is an anti-correlation relation between their central densities and pericenters [33], which seems to support this scenario.

In this *Letter*, we explore tidal evolution of SIDM subhalos in the MW's tides, using N-body simulations implemented with realistic MW potentials. The SIDM thermalization coupled with the MW tidal field can lead to diverse dark matter distributions in subhalos. And they can be in either core-collapse or -expansion phases, depending on the cross section, pericenter and initial halo concentration. We demonstrate that Draco and Fornax, two extremes in the dark matter content among the bright MW dSphs, can be explained in the SIDM model with $\sigma/m = 3 \text{ cm}^2/\text{g}$, the value used to fit the diverse rotation curves of spiral galaxies in the field [9, 24, 25]. We further explicitly show the mechanism leading to core collapse in the tidal field and study mass loss for both SIDM and CDM subhalos.

Simulation setup. We carry out N-body simulations using the code AREPO [45] with a module developed in [14] for modeling dark matter self-interactions, and use SUBFIND [45] to follow the evolutionary track of the subhalo, defined as the set of gravitationally self-bound particles. Following [20], we model the baryon and dark matter distributions of the MW with static potentials, while treating dwarf subhalos with the N-body code.

We include both the disk and bulge components in our MW model since they present in the MW and can play a significant role in tidal evolution of the subhalos [42].

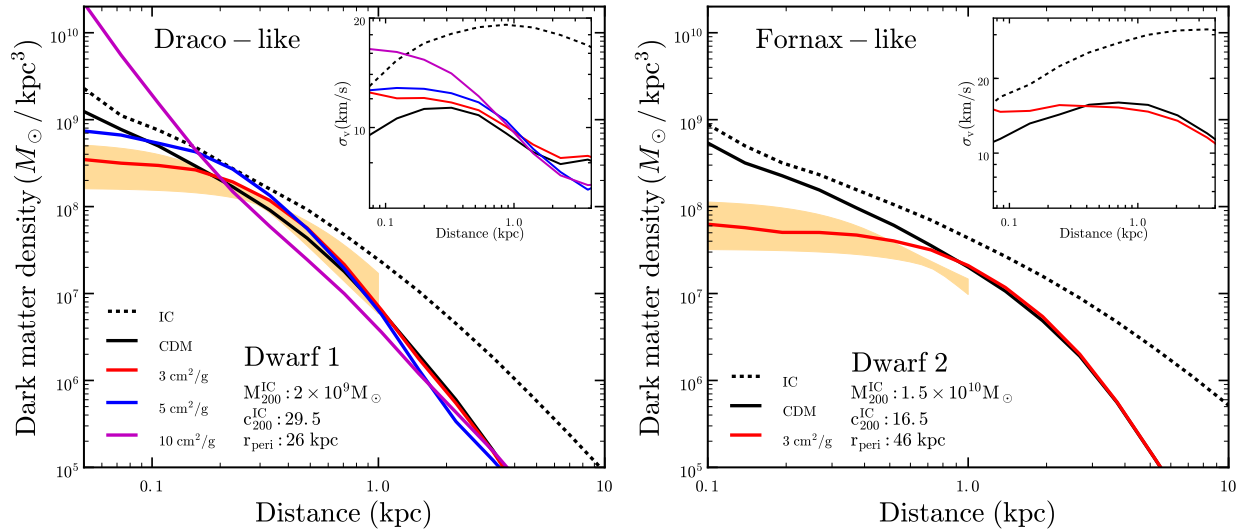


FIG. 1. Dark matter density and velocity-dispersion (inset) profiles at $t = 10$ Gyr for Dwarf 1 (left) and Dwarf 2 (right). The orange bands show cored isothermal density profiles from the fits to stellar kinematics of Draco (left) and Fornax (right) at 95% CL [33].

For the stellar disk, we use the Miyamoto-Nagai potential $\Phi_{\text{MN}} = -GM_{\text{d}}/\sqrt{R^2 + (R_{\text{d}} + \sqrt{z_{\text{d}}^2 + z^2})^2}$ [46], where $M_{\text{d}} = 6.98 \times 10^{10} M_{\odot}$ is the disk mass, $R_{\text{d}} = 3.38$ kpc is the disk scale length, and $z_{\text{d}} = 0.3$ kpc is the disk scale height. In addition, we include a Hernquist bulge potential $\Phi_{\text{H}} = -GM_{\text{H}}/(r+r_{\text{H}})$ [47], where $M_{\text{H}} = 1.05 \times 10^{10} M_{\odot}$ is the bulge mass and $r_{\text{H}} = 0.46$ kpc. We model the main halo using an NFW profile [48] with the maximal velocity $V_{\text{max}} = 200.5$ km/s and the associated radius $r_{\text{max}} = 43.4$ kpc, and the corresponding halo mass is $M_{200} = 1.4 \times 10^{12} M_{\odot}$. With these parameters chosen for the main halo and the baryonic component, we can reproduce the MW mass model presented in [49], in accord with measurements of MW stellar kinematics and the local dark matter density. In principle, one should also include the self-scattering effect for the main halo. However, for a MW-like galaxy, where the baryons dominate the central regions, an SIDM halo profile can be similar to an NFW one, because SIDM thermalization with the baryonic potential increases the central dark matter density [16, 18, 20, 42]. We have checked that the NFW halo we take here is a good approximation to the SIDM MW halo constructed in [20]. We also note that the host potential does not evolve with time.

We use an NFW profile to model the initial dark matter distribution in subhalos and choose the following three sets of initial conditions. Dwarf 1: its characteristic maximal circular velocity and associated radius are $V_{\text{max}} = 28.8$ km/s and $R_{\text{max}} = 1.9$ kpc, respectively. And the corresponding halo mass is $M_{200} = 2 \times 10^9 M_{\odot}$ and concentration $c_{200} = 29.5$, evaluated at redshift 0; Dwarf 2: $V_{\text{max}} = 47.6$ km/s and $R_{\text{max}} = 6.8$ kpc, or equivalently $M_{200} = 1.5 \times 10^{10} M_{\odot}$ and $c_{200} = 16.5$; Dwarf 3: $V_{\text{max}} = 26.7$ km/s and $R_{\text{max}} = 2.5$ kpc, or

$M_{200} = 2 \times 10^9 M_{\odot}$ and $c_{200} = 22.9$. Note Dwarf 3 has the same initial halo mass as Dwarf 1, but its concentration is slightly lower. We use the code SPHERIC [50] to generate initial conditions for the subhalos.

For Dwarf 1 and 3, we simulate CDM and SIDM cases with $\sigma/m = 3$ cm²/g, 5 cm²/g and 10 cm²/g, and fix the pericenter as 26.5 kpc to be consistent with Draco’s, 28_{-7}^{+12} kpc, estimated from Gaia DR 2 [44]. For Dwarf 2, we perform the CDM run as well as SIDM with $\sigma/m = 3$ cm²/g, and take the pericenter as 46 kpc, motivated by Fornax’s 58_{-18}^{+26} kpc [44]. We place the initial subhalo at a distance of 230 kpc from the center of the main halo at $t = 0$, and confine the orbit in the plane of the stellar disk. For each subhalo, we choose a “kick” velocity, which is perpendicular to the line connecting the center of the main halo and the subhalo, so that we can obtain the desired pericenter distance; see Appendix for the orbital trajectory of Dwarf 1. We perform simulations with total number of particles $N_{\text{p}} = 10^6$ for Dwarf 1 and 3, and $N_{\text{p}} = 5 \times 10^6$ for Dwarf 2, yielding equivalent-Plummer gravitational softening length of 25 pc.

A case for Draco and Fornax. We first highlight that the SIDM model with a fixed cross section could explain both Draco and Fornax, although their central dark matter densities differ significantly.

Fig. 1 (left) shows the density and velocity-dispersion profiles (solid) at $t = 10$ Gyr for Dwarf 1. In all cases, the MW’s tides significantly strip away halo masses and lower densities in the outer regions. All of them have similar density profiles for $r \gtrsim 1$ kpc, but their central densities are different. For CDM, the inner profile is resilient to tidal stripping and remains cuspy as the initial one (dashed), consistent with earlier findings [34–36]. While for SIDM, the central density increases with

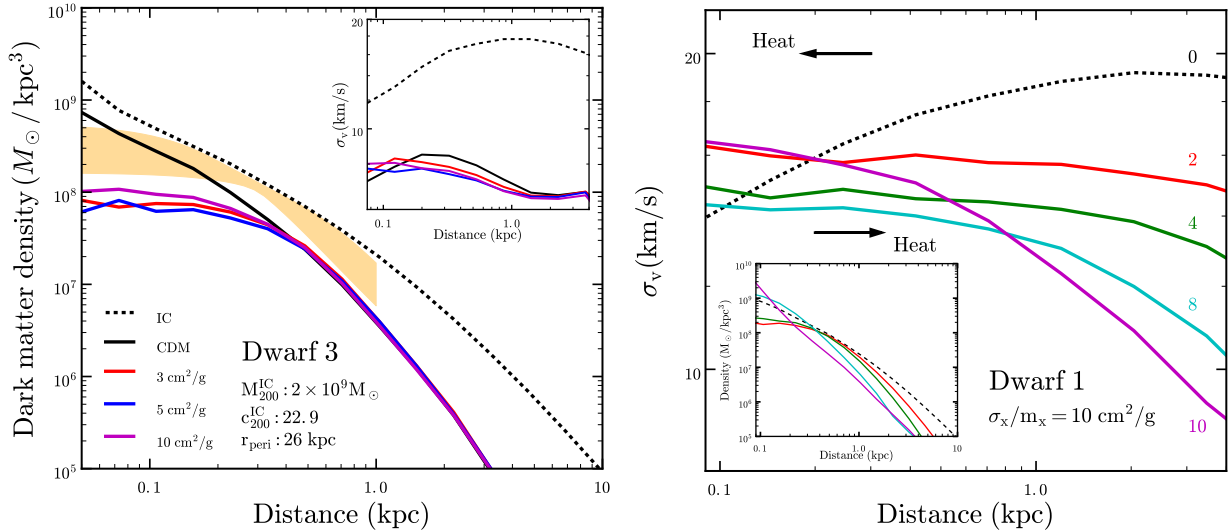


FIG. 2. Left: Dark matter density and velocity-dispersion (inset) profiles for Dwarf 3. It has the same initial mass as Dwarf 1, but slightly lower concentration. The orange band is the same as the left panel of Fig. 1. Right: dark matter velocity-dispersion and density (inset) profiles at different evolution times, $t = 0, 2, 4, 8$ and 10 Gyr for Dwarf 1 with $\sigma/m = 10 \text{ cm}^2/\text{g}$. The symbol “ \leftarrow ” (“ \rightarrow ”) denotes the heat-flow direction in the SIDM core-expansion (-collapse) phase.

the cross section, opposite to the trend found in field halos [30, 51]. In fact, all the SIDM halos are in the core-collapse phase after 10 Gyr’s tidal evolution, as their velocity dispersions are larger than the CDM counterpart and profiles have negative gradients in the inner regions, $r \lesssim 1$ kpc, an indication of SIDM core collapse [43, 51–53]. For a field halo with the same halo parameters as Dwarf 1, we can use equation 4 in [53] to estimate the core-collapse time to be $t_c \sim 16$ Gyr for $\sigma/m = 10 \text{ cm}^2/\text{g}$ and it becomes even longer for a smaller cross section, as $t_c \propto 1/(\sigma/m)$. Thus, the MW tides can significantly accelerate the onset of core collapse for SIDM subhalos.

For SIDM with $\sigma/m = 3 \text{ cm}^2/\text{g}$, the dark matter density profile after tidal evolution agrees with the cored isothermal density profile inferred from the stellar kinematics of Draco [33]. For a field halo with the same initial NFW profile as Dwarf 1, dark matter self-interactions create a large density core and the central density is $8.5 \times 10^7 M_{\odot}/\text{kpc}^3$ estimated using the analytical model in [23], too low to be consistent with observations of Draco. This explains why the earlier analyses [29, 32], which did not take into account the tidal effects, found $\sigma/m \lesssim 0.3 \text{ cm}^2/\text{g}$ for Draco. While for two other SIDM simulations with larger cross sections, the predicted central densities are actually too high to explain Draco, opposite to the expectation for the field halo. We have also checked that for Dwarf 1 with $\sigma/m = 3 \text{ cm}^2/\text{g}$, the inner density is reduced by 20% if we allow for pre-evolution for 3 Gyr outside of the main halo and then another 10 Gyr’s tidal evolution.

Fig. 1 (right) shows the density and velocity-dispersion profiles at $t = 10$ Gyr for Dwarf 2. We take

$\sigma/m = 3 \text{ cm}^2/\text{g}$ for the SIDM run, and the halo is still in the core-expansion phase after 10 Gyr’s evolution. Dwarf 2 has higher halo initial mass but lower concentration, compared to Dwarf 1. In this case, the interplay between dark matter self-interactions and gravitational tides leads to a large SIDM density core and a shallow density profile, reproducing the cored density profile inferred from Fornax [33] reasonably well. We could adjust its halo parameters and pericenter to further improve the agreement in the range of 0.5 – 1 kpc.

We have demonstrated that the interplay between SIDM thermalization and tidal stripping can lead to diverse central densities for subhalos, in accord with observations. Draco’s host has high concentration and experiences core collapse when it evolves in the MW’s tidal field, resulting in a high central density. On the other hand, Fornax’s host halo concentration is lower, and it is in the core-expansion phase after tidal evolution, leading to a shallow density core. Thus, we expect SIDM can accommodate diverse dark matter contents in MW dSphs, as we have shown for the two extremes, Draco and Fornax, consistent with theoretical predictions [33, 43]. In our simulations, we have deliberately chosen the halo parameters for Dwarf 1 and 2 such that the SIDM model with $\sigma/m = 3 \text{ cm}^2/\text{g}$ [9, 24, 25] can reproduce the observations after the tidal evolution. For other σ/m values, we would need to adjust the initial parameters to match observations.

Dwarf 1’s initial halo concentration is on the higher end of the distribution predicted in cosmological simulations [54], but we emphasize this is a necessary condition for the core collapse to occur, as t_c is extremely sensitive to c_{200} [33, 43, 53], $t_c \propto (\sigma/m)^{-1} M_{200}^{-1/3} c_{200}^{-7/2}$. A

small difference in c_{200} could lead to a huge difference in t_c . To see this, we simulate Dwarf 3 that has the same initial mass as Dwarf 1 but slightly lower concentration. As shown in Fig. 2 (left), all SIDM cases have similar shallow density profiles and there is no clear evidence of core collapse, even though c_{200} is only reduced by 20%. In this case, even CDM predicts a density too low to be consistent with observations for $r \gtrsim 0.2$ kpc, indicating that Draco’s host could be indeed highly-concentrated. On the other hand, since there is a degeneracy between t_c and σ/m , one may reduce c_{200} mildly by increasing σ/m . In addition, smaller c_{200} could be allowed if the actual pericenter distance is smaller than the one we take in simulations.

Tidal evolution and core collapse. To further appreciate dynamics triggering SIDM core collapse in the tidal field, we take a close look at the evolution history of Dwarf 1 with $\sigma/m = 10$ cm²/g, the most extreme case in our study.

Fig. 2 (right) shows the velocity-dispersion profiles at different times during the evolution. Overall, the σ_v value at large radii, say $r = 1$ kpc, decreases gradually, due to tidal stripping from the MW. Initially, inner σ_v has a positive gradient in the radius as predicted by the NFW profile. At early stages of the evolution, dark matter self-interactions lead to heat transfer from the outer to inner regions, denoted by the “←” symbol, the core size increases and the central density decreases, similar to the case of a field SIDM halo. At the same time, the maximal value of σ_v , the height of the heat reservoir of the dwarf halo, decreases over time due to the mass loss of the dwarf halo in the MW tidal field. Thus, a negative gradient, a necessary condition for the onset of SIDM core collapse, can be more easily satisfied for a subhalo than a field halo. For the example we consider, the transition occurs around 4 Gyr, at a time when the inner dispersion profile is almost flat. Then, the heat flow reverses its direction towards the outer region (“→”). As a self-gravitating system, the inner halo has negative heat capacity, the more heat is extracted by dark matter collisions, the further it collapses to convert its gravitational energy to kinetic energy [55]. Thus, both the inner dispersion and density increases at late stages, $t = 8$ –10 Gyr. We have also simulated Dwarf 1 with $\sigma/m = 10$ cm²/g, but a larger pericenter, 46 kpc, and found the core-collapse transition occurs around 8 Gyr.

Mass loss. As we have shown, the interplay between dark matter self-interactions and the MW’s tides can lead to diverse inner density profiles. However, overall tidal evolution histories for the cases we consider are remarkably similar. Fig. 3 shows the ratio of the total mass of bound particles to the initial halo mass vs. time. For CDM and SIDM ($\sigma/m = 3$ cm²/g) simulations of Dwarf 1, we present high-frequency time output results, while low-frequency ones for the others. In all

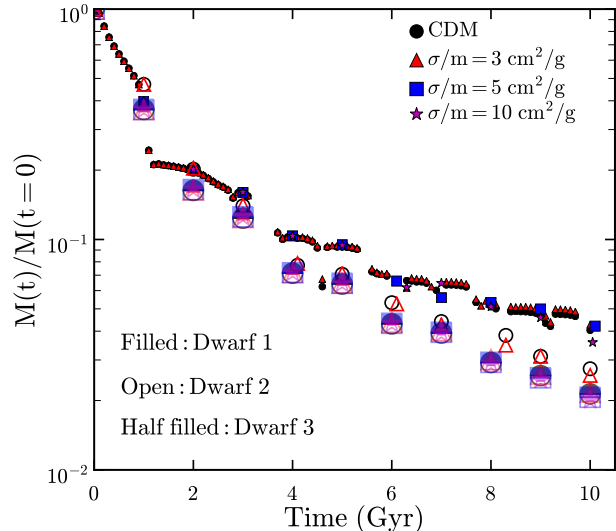


FIG. 3. Time evolution of the bound mass, normalized to the initial halo mass.

cases, the halo loses 80% of its initial mass within the first 2 Gyr. Moreover, for a given initial halo and its pericenter, the mass loss rate is almost independent of the self-scattering cross section for the cases we study.

We also find that the mass-loss rate is sensitive to the halo concentration. For example, Dwarf 1 has a smaller pericenter than Dwarf 2, but its mass-loss rate at later stages is less pronounced than Dwarf 2. And Dwarf 1 and Dwarf 3 have the same pericenter and initial mass, but the former is a factor of 2 more massive than the later after $t = 10$ Gyr’s tidal evolution as Dwarf 1 has a higher initial c_{200} value. These results reflect the fact that a subhalo with high concentration is more resilient to tidal stripping.

Conclusions. We have shown that the interaction between the SIDM subhalos and the MW’s tides can lead to diverse dark matter density profiles in the inner region. The significance of the tidal effects depends on several factors, including the subhalo concentration, mass, self-scattering cross section, pericenter and infall time. In particular, our simulations show the SIDM core-collapse condition is extremely sensitive to the initial halo concentration. After including the tidal effects, we have demonstrated that the SIDM model with a fixed cross section, proposed for field galaxies, can accommodate the MW dSphs Draco and Fornax as well, although their dark matter contents differ significantly. For the cases we studied, the overall mass loss rates are almost identical for SIDM and CDM subhalos. With our choice of orbits, all simulated dwarf halos lose 96–98% of their original mass after 10 Gyr’s tidal evolution.

There are several promising directions we can explore in the future. It is natural to extend our work to other MW dwarfs, including ultra-faint dwarf galaxies, to see if SIDM can fully reproduce the observed trends in these

systems [33]. Moreover, we can study the stellar distribution of MW dwarf galaxies and its correlation with the core size and the pericenter. It would also be of great interest to perform hydrodynamical simulations to follow the formation and growth of a MW-like galaxy and study the tidal effects on SIDM subhalos in the cosmological setup.

Acknowledgements: We thank Manoj Kaplinghat, Matthew Walker and Mauro Valli for useful discussion, and Volker Springel for making AREPO available for this work. OS acknowledges support from NASA MUREP Institutional Opportunity (MIRO) grant number NNX15AP99A and thanks the Carnegie Observatories for hospitality during the completion of this work. HBY acknowledges support from U.S. Department of Energy under Grant No. de-sc0008541 and UCR Regents' Faculty Development Award. LVS is grateful for support from the Hellman Fellow Foundation. MV acknowledges support through an MIT RSC award, a Kavli Research Investment Fund, NASA ATP grant NNX17AG29G, NSF grants AST-1814053 and AST-1814259. JZ acknowledges support by a Grant of Excellence from the Icelandic Research Fund (grant number 173929-051). Part of the simulations was run on the Comet supercomputer at the San Diego Supercomputer Center, which is funded by the National Science Foundation award #OAC-#1341698.

REFERENCES

- * osame001@ucr.edu
- [1] P. A. R. Ade *et al.* (Planck), *Astron. Astrophys.* **594**, A13 (2016), arXiv:1502.01589 [astro-ph.CO].
 - [2] S. Trujillo-Gomez, A. Klypin, J. Primack, and A. J. Romanowsky, *Astrophys. J.* **742**, 16 (2011), arXiv:1005.1289 [astro-ph.CO].
 - [3] M. Vogelsberger, S. Genel, V. Springel, P. Torrey, D. Sijacki, D. Xu, G. F. Snyder, S. Bird, D. Nelson, and L. Hernquist, *Nature* **509**, 177 (2014), arXiv:1405.1418 [astro-ph.CO].
 - [4] M. Vogelsberger, S. Genel, V. Springel, P. Torrey, D. Sijacki, D. Xu, G. Snyder, D. Nelson, and L. Hernquist, **444**, 1518 (2014), arXiv:1405.2921.
 - [5] S. Tulin and H.-B. Yu, (2017), arXiv:1705.02358 [hep-ph].
 - [6] J. S. Bullock and M. Boylan-Kolchin, *Ann. Rev. Astron. Astrophys.* **55**, 343 (2017), arXiv:1707.04256 [astro-ph.CO].
 - [7] K. A. Oman *et al.*, *Mon. Not. Roy. Astron. Soc.* **452**, 3650 (2015), arXiv:1504.01437 [astro-ph.GA].
 - [8] S. McGaugh, F. Lelli, and J. Schombert, *Phys. Rev. Lett.* **117**, 201101 (2016), arXiv:1609.05917 [astro-ph.GA].
 - [9] T. Ren, A. Kwa, M. Kaplinghat, and H.-B. Yu, (2018), arXiv:1808.05695 [astro-ph.GA].
 - [10] D. N. Spergel and P. J. Steinhardt, *Phys. Rev. Lett.* **84**, 3760 (2000), arXiv:astro-ph/9909386 [astro-ph].
 - [11] R. Dave, D. N. Spergel, P. J. Steinhardt, and B. D. Wandelt, *Astrophys. J.* **547**, 574 (2001), arXiv:astro-ph/0006218 [astro-ph].
 - [12] M. Rocha, A. H. G. Peter, J. S. Bullock, M. Kaplinghat, S. Garrison-Kimmel, J. Onorbe, and L. A. Moustakas, *Mon. Not. Roy. Astron. Soc.* **430**, 81 (2013), arXiv:1208.3025 [astro-ph.CO].
 - [13] A. H. G. Peter, M. Rocha, J. S. Bullock, and M. Kaplinghat, *Mon. Not. Roy. Astron. Soc.* **430**, 105 (2013), arXiv:1208.3026 [astro-ph.CO].
 - [14] M. Vogelsberger, J. Zavala, and A. Loeb, *Mon. Not. Roy. Astron. Soc.* **423**, 3740 (2012), arXiv:1201.5892 [astro-ph.CO].
 - [15] M. Vogelsberger, J. Zavala, K. Schutz, and T. R. Slatyer, **484**, 5437 (2019), arXiv:1805.03203.
 - [16] M. Kaplinghat, R. E. Keeley, T. Linden, and H.-B. Yu, *Phys. Rev. Lett.* **113**, 021302 (2014), arXiv:1311.6524 [astro-ph.CO].
 - [17] M. Vogelsberger, J. Zavala, C. Simpson, and A. Jenkins, *Mon. Not. Roy. Astron. Soc.* **444**, 3684 (2014), arXiv:1405.5216 [astro-ph.CO].
 - [18] O. D. Elbert, J. S. Bullock, M. Kaplinghat, S. Garrison-Kimmel, A. S. Graus, and M. Rocha, *Astrophys. J.* **853**, 109 (2018), arXiv:1609.08626 [astro-ph.GA].
 - [19] A. Robertson *et al.*, *Mon. Not. Roy. Astron. Soc.* **476**, L20 (2018), arXiv:1711.09096 [astro-ph.CO].
 - [20] O. Sameie, P. Creasey, H.-B. Yu, L. V. Sales, M. Vogelsberger, and J. Zavala, *Mon. Not. Roy. Astron. Soc.* **479**, 359 (2018), arXiv:1801.09682 [astro-ph.GA].
 - [21] A. Robertson, D. Harvey, R. Massey, V. Eke, I. G. McCarthy, M. Jauzac, B. Li, and J. Schaye, (2018), arXiv:1810.05649 [astro-ph.CO].
 - [22] A. Fitts, M. Boylan-Kolchin, B. Bozek, J. S. Bullock, A. Graus, V. Robles, P. F. Hopkins, K. El-Badry, S. Garrison-Kimmel, C.-A. Faucher-Giguère, A. Wetzel, and D. Kereš, arXiv e-prints (2018), arXiv:1811.11791.
 - [23] M. Kaplinghat, S. Tulin, and H.-B. Yu, *Phys. Rev. Lett.* **116**, 041302 (2016), arXiv:1508.03339 [astro-ph.CO].
 - [24] A. Kamada, M. Kaplinghat, A. B. Pace, and H.-B. Yu, *Phys. Rev. Lett.* **119**, 111102 (2017), arXiv:1611.02716 [astro-ph.GA].
 - [25] P. Creasey, O. Sameie, L. V. Sales, H.-B. Yu, M. Vogelsberger, and J. Zavala, *Mon. Not. Roy. Astron. Soc.* **468**, 2283 (2017), arXiv:1612.03903 [astro-ph.GA].
 - [26] M. Boylan-Kolchin, J. S. Bullock, and M. Kaplinghat, *Mon. Not. Roy. Astron. Soc.* **415**, L40 (2011), arXiv:1103.0007 [astro-ph.CO].
 - [27] M. Boylan-Kolchin, J. S. Bullock, and M. Kaplinghat, *Mon. Not. Roy. Astron. Soc.* **422**, 1203 (2012), arXiv:1111.2048 [astro-ph.CO].
 - [28] J. Zavala, M. Vogelsberger, and M. G. Walker, *Mon. Not. Roy. Astron. Soc.* **431**, L20 (2013), arXiv:1211.6426 [astro-ph.CO].
 - [29] M. Valli and H.-B. Yu, *Nat. Astron.* **2**, 907 (2018), arXiv:1711.03502 [astro-ph.GA].
 - [30] M. Vogelsberger, J. Zavala, F.-Y. Cyr-Racine, C. Pfrommer, T. Bringmann, and K. Sigurdson, *Mon. Not. Roy. Astron. Soc.* **460**, 1399 (2016), arXiv:1512.05349 [astro-ph.CO].
 - [31] J. I. Read, M. G. Walker, and P. Steger, *Mon. Not. Roy. Astron. Soc.* ”**484**”, ”1401 (2019), arXiv:1808.06634 [astro-ph.GA].
 - [32] J. I. Read, M. G. Walker, and P. Steger, *Mon. Not. Roy. Astron. Soc.* **481**, 860 (2018), arXiv:1805.06934 [astro-ph.GA].

- [33] M. Kaplinghat, M. Valli, and H.-B. Yu, (2019), arXiv:1904.04939 [astro-ph.GA].
- [34] E. Hayashi, J. F. Navarro, J. E. Taylor, J. Stadel, and T. R. Quinn, *Astrophys. J.* **584**, 541 (2003), arXiv:astro-ph/0203004 [astro-ph].
- [35] J. Peñarrubia, J. F. Navarro, and A. W. McConnachie, *Astrophys. J.*
- [36] J. Peñarrubia, A. J. Benson, M. G. Walker, G. Gilmore, A. W. McConnachie, and L. Mayer, *Mon. Not. Roy. Astron. Soc.* **406**, 1290 (2010), arXiv:1002.3376.
- [37] A. M. Brooks and A. Zolotov, *Astrophys. J.* **786**, 87 (2014), arXiv:1207.2468 [astro-ph.CO].
- [38] A. R. Wetzel, P. F. Hopkins, J.-h. Kim, C.-A. Faucher-Giguère, D. Kereš, and E. Quataert, *The Astrophysical Journal, Letters* **827**, L23 (2016), arXiv:1602.05957.
- [39] T. Sawala *et al.*, *Mon. Not. Roy. Astron. Soc.* **457**, 1931 (2016), arXiv:1511.01098 [astro-ph.GA].
- [40] A. Fattahi, J. F. Navarro, T. Sawala, C. S. Frenk, L. V. Sales, K. Oman, M. Schaller, and J. Wang, (2016), arXiv:1607.06479 [astro-ph.GA].
- [41] S. Garrison-Kimmel, A. Wetzel, J. S. Bullock, P. F. Hopkins, M. Boylan-Kolchin, C.-A. Faucher-Giguère, D. Kereš, E. Quataert, R. E. Sanderson, A. S. Graus, and T. Kelley, *Mon. Not. Roy. Astron. Soc.* **471**, 1709 (2017), arXiv:1701.03792.
- [42] V. H. Robles, T. Kelley, J. S. Bullock, and M. Kaplinghat, (2019), arXiv:1903.01469 [astro-ph.GA].
- [43] H. Nishikawa, K. K. Boddy, and M. Kaplinghat, (2019), arXiv:1901.00499 [astro-ph.GA].
- [44] T. K. Fritz, G. Battaglia, M. S. Pawłowski, N. Kallivayalil, R. van der Marel, S. T. Sohn, C. Brook, and G. Besla, *Astronomy & Astrophysics* **619**, A103 (2018), arXiv:1805.00908 [astro-ph.GA].
- [45] V. Springel, N. Yoshida, and S. D. M. White, *New Astron.* **6**, 79 (2001), arXiv:astro-ph/0003162 [astro-ph].
- [46] M. Miyamoto and R. Nagai, *PASP* **27**, 533 (1975).
- [47] L. Hernquist, *Astrophys. J.* **356**, 359 (1990).
- [48] J. F. Navarro, C. S. Frenk, and S. D. M. White, *Astrophys. J.* **462**, 563 (1996), arXiv:astro-ph/9508025 [astro-ph].
- [49] P. J. McMillan, *Mon. Not. Roy. Astron. Soc.* **414**, 2446 (2011), arXiv:1102.4340 [astro-ph.GA].
- [50] S. Garrison-Kimmel, M. Rocha, M. Boylan-Kolchin, J. Bullock, and J. Lally, *Mon. Not. Roy. Astron. Soc.* **433**, 3539 (2013), arXiv:1301.3137 [astro-ph.CO].
- [51] O. D. Elbert, J. S. Bullock, S. Garrison-Kimmel, M. Rocha, J. Onorbe, and A. H. G. Peter, *Mon. Not. Roy. Astron. Soc.* **453**, 29 (2015), arXiv:1412.1477 [astro-ph.GA].
- [52] S. Balberg, S. L. Shapiro, and S. Inagaki, *Astrophys. J.* **568**, 475 (2002), arXiv:astro-ph/0110561 [astro-ph].
- [53] R. Essig, H.-B. Yu, Y.-M. Zhong, and S. D. McDermott, (2018), arXiv:1809.01144 [hep-ph].
- [54] S. V. Pilipenko, M. A. Sánchez-Conde, F. Prada, and G. Yepes, *Mon. Not. Roy. Astron. Soc.* **472**, 4918 (2017), arXiv:1703.06012 [astro-ph.CO].
- [55] J. Binney and S. Tremaine, *Galactic Dynamics: Second Edition*, by James Binney and Scott Tremaine. ISBN 978-0-691-13026-2 (HB). Published by Princeton University Press, Princeton, NJ USA, 2008. (Princeton University Press, 2008).

Appendix: Orbital trajectory

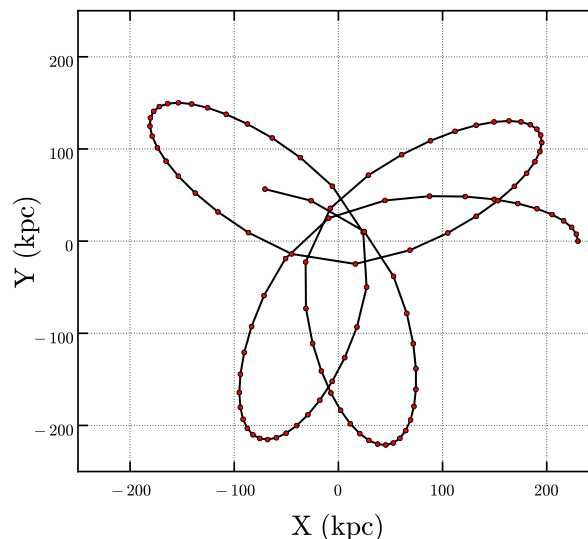


FIG. 4. Orbital trajectory for Dwarf 1 with $\sigma/m = 3 \text{ cm}^2/\text{g}$.

Fig. 4 shows the orbital trajectory for Dwarf 1, which has a pericenter of 26 kpc. In our simulations, we place the initial subhalo at a distance of 230 kpc from the center of the main halo and confine the orbit in the plane of the disk.